Received: 16 December 2016 | Accepted: 20 June 2017

DOI: 10.1002/rnc.3890

RESEARCH ARTICLE

WILEY

Fast terminal sliding-mode finite-time tracking control with differential evolution optimization algorithm using integral chain differentiator in uncertain nonlinear systems

Ruizi Ma[1] | Guoshan Zhang[1] | Olav Krause[2]

[1]School of Electrical Engineering and Automation, Tianjin University, Tianjin, China

[2]School of Information Technology and Electrical Engineering, The University of Queensland, Brisbane, Queensland, Australia

Correspondence
Ruizi Ma, School of Electrical Engineering and Automation, Tianjin University, No.92, Weijin Road, Nankai District, Tianjin, 300072, China
Email: maruiziran@163.com

Funding information
National Natural Science Foundation of China, Grant/Award Number: 61473202

Summary

This paper presents a fast terminal sliding-mode tracking control for a class of uncertain nonlinear systems with unknown parameters and system states combined with time-varying disturbances. Fast terminal sliding-mode finite-time tracking systems based on differential evolution algorithms incorporate an integral chain differentiator (ICD) to feedback systems for the estimation of the unknown system states. The differential evolution optimization algorithm using ICD is also applied to a tracking controller, which provides unknown parametric estimation in the limitation of unknown system states for trajectory tracking. The ICD in the tracking systems strengthens the tracking controller robustness for the disturbances by filtering noises. As a powerful finite-time control effort, the fast terminal sliding-mode tracking control guarantees that all tracking errors rapidly converge to the origin. The effectiveness of the proposed approach is verified via simulations, and the results exhibit high-precision output tracking performance in uncertain nonlinear systems.

KEYWORDS

differential evolution, differentiator, nonlinear systems, terminal sliding mode, tracking

1 | INTRODUCTION

Sliding-mode control (SMC) is an efficient control scheme and has been widely applied in nonlinear systems. Sliding-mode control has many attractive features such as insensitivity to the model errors and parametric uncertainties.[1,2] Given its advantages, SMC provides powerful techniques to complicated nonlinear dynamic systems for tracking control, including robotic manipulator systems,[3] active suspension vehicle systems,[4] induction motor drive systems,[5,6] power systems,[7] and spacecraft systems.[8]

The tracking problems using evolutionary optimization in complicated nonlinear systems attract much more attention. Evolutionary optimization algorithms are considered as a powerful optimization tool in solving nonlinear and complicated search spaces.[9] Sliding-mode control combined with evolutionary optimization algorithms is presented to improve the tracking performances for complicated nonlinear systems, such as genetic algorithms[10] and particle swarm algorithms.[11,12] These methods have difficulty solving a class of nonlinear tracking problems of unknown system states with time-varying disturbances, which causes an impact on the convergence and stability of the tracking systems.

In limited situations, the system states are unknown and needs to be estimated. Along with time-varying disturbances, the differential evolution (DE) optimization algorithm using an integral chain differentiator (ICD) proposed in

this paper is introduced into the design of a sliding-mode tracking controller to produce continuous state estimations by relying only on the position measurements. Compared with other intelligent optimization algorithms, faster convergence properties and accurate search performances are obtained from the DE optimization algorithm.[13-15] A DE optimization scheme is advantageous because it only needs a few control parameters to be defined, which is appropriate for nonlinear constrained optimization problems. Because of its favorable performance, the DE algorithm has numerous applications in the control of tunnel responses,[16] robot path planning,[17] permanent magnet synchronous motors,[18] and chaotic systems.[19]

Tracking performance optimization is studied extensively in finite-time control related to the technique work demonstrated by Li et al,[20] and the advantages of finite-time tracking control are fast convergence properties in high accuracy within the origin areas. Terminal SMC (TSMC) was developed to guarantee finite-time optimization control by introducing nonlinear sliding-mode manifolds.[21] Compared with the conventional SMC, TSMC is an effective finite-time control and converges faster when states approach the origin in higher precision.[22] Particularly, TSMC closed-loop systems have a non-Lipschitz property, which is similar to dynamic systems by finite-time control based on the homogeneous theory.[23] The advantages shown are powerful in solving the tracking problems of uncertainty in dynamic systems. Terminal SMCs have been applied in robot control,[24] power system control,[25] and motor control[26] and other industrial complicated systems with uncertainties.

The drawbacks of the methods referred above are that TSMC stability is guaranteed within the prescribed set of uncertainties and fast and precise tracking techniques are unavailable for unknown system states with time-varying disturbances and unknown parameters in nonlinear uncertain systems, which exaggerates the oscillation and influences tracking precision and stability in the nonlinear uncertain systems. The development of a differentiator technique provides an effective method for state estimation. The problem of unmeasured system states in the tracking control is solved by the derivative computation of available measured output signals. The ICD is capable of using a first-order signal to estimate other high-order signals accurately. The high-order ICD achieves a satisfactory tracking performance and accurate differential estimation without relying on model information applicable in engineering.[27] For example, Wang et al[28] used a singular perturbation technique to design a finite-time convergent differentiator that reduces chattering phenomena. A back-stepping trajectory tracking control technique-based differentiator is proposed for hypersonic reentry vehicles.[29] Additionally, the filter function of ICD restrains the disturbances, eliminating the effects of disturbances to stability and accuracy. Meanwhile, fast TSMC (FTSMC), which preserves the main features of the TSMC, keeps robustness to time-varying disturbances and provides faster finite-time convergence without excessive control effort. Given the fast finite-time convergence property, the development of FTSMC is shown in a wide range of complicated real applications, such as unmanned aerial vehicles,[30] piezoelectric plates,[31] and direct current–direct current boost converter[32] for accurate tracking control.

To overcome the above-mentioned limitations of the tracking techniques, this paper proposes an FTSMC-based DE optimization algorithm using ICD (FTSMC-DD) to realize the precision tracking control for unknown parameters and states in nonlinear systems with time-varying disturbances. The DE optimization algorithm using ICD removes the restriction of parametric estimation in lacking state information. The feedback tracking system added into the ICD achieves an accurate estimation of unknown system states. The ICD is also used to reduce the chattering effects, which has the characteristics of filtering noisy signals and having a simple structure. The application of ICD strengthens the tracking property on the basis of the filter function under the time-varying disturbances and enhances the FTSMC's accurate tracking ability. The Lyapunov synthesis based on stability analysis is used to prove that all the output signals in the closed-loop systems converged to the desired trajectory with tracking errors converging to the origin. The analysis of finite-time stability is presented to verify that dynamic system states converge to an equilibrium state in finite time. The proposed algorithm reduces the tracking errors and chattering effects, achieving high-precision tracking performance.

The paper is organized as follows. In Section 2, the description of uncertain nonlinear systems is given. In Section 3, the fast terminal sliding-mode finite-time tracking control based on the DE algorithm with ICD is demonstrated. The effectiveness of the proposed approach is verified in Section 4. Finally, some conclusions are drawn in Section 5.

2 | PROBLEM FORMULATION

This paper considers the following second-order nonlinear system with unknown parameters and states described by

$$\begin{aligned} \dot{x}_1(t) &= x_2(t), \\ \dot{x}_2(t) &= f(\theta, x) + g(\xi, x)u(t) + d(t), \\ y(t) &= x_1(t), \end{aligned} \tag{1}$$

where $x = [x_1, x_2]^T$ is a state vector; x_2 is an unknown system state; $y(t)$ is the system output; control input $u(t)$ is bounded; $f(\theta, x)$ and $g(\xi, x)$ are nonlinear functions; $g(\xi, x) \neq 0$, $\theta = [\theta_1\theta_2\cdots\theta_{\bar{s}}]^T$, and $\xi = [\xi_1\xi_2\cdots\xi_{\bar{q}}]^T$ are the unknown parameter vectors; θ_i, $i = 1, 2, 3, ..., \bar{s}$, and ξ_i, $i = 1, 2, 3, ..., \bar{q}$, are unknown parameters; $d(t)$ is the time-varying ;disturbances and $|d(t)| \leq L_d$.

The control objective is to design the fast terminal sliding-mode controller $u(t)$ for the uncertain nonlinear system to complete the target that output tracks the desired trajectory with a prescribed accuracy μ, which is a sufficiently small constant as follows:

$$|y(t)-y_d(t)|\leq\mu,$$

Thus, we introduce the error states given by

$$e_i(t) = x_i(t)-y_d{}^{(i-1)}(t), \quad i = 1, 2,$$

where $e_1 = x_1 - y_d$ is the tracking error and y_d is the reference signal. Hence, the error dynamics are given by

$$\begin{aligned}\dot{e}_1(t) &= e_2(t),\\ \dot{e}_2(t) &= f(\theta, x) + g(\xi, x)u(t) + d(t)-y_d^{(2)}.\end{aligned} \tag{2}$$

Next, consider a vector $\hat{e}$ as

$$\hat{e}(t) = [\hat{e}_1(t), \quad \hat{e}_2(t)]^T = \left[\hat{x}_1(t)-y_d, \quad \hat{x}_2(t)-y_d^{(1)}\right]^T,$$

where $\hat{e} \in R^2$ and $\hat{x}_i$, $i = 1, 2$, is the estimation states.

Terminal SMC exhibits finite-time convergence to the origin with a nonlinear sliding-mode variable.[21] The tracking surface function on the basis of the conventional TSMC[33] is defined as

$$\sigma = e_2 + \beta e_1^{\frac{q}{p}}, \tag{3}$$

where $\beta > 0$ is the sliding-mode parameter, p and q are the positive odd integers satisfying $0 < q < p$. The sufficient condition for the existence of the prescribed sliding-mode surface[34] is

$$\frac{d\sigma^2}{dt}<-\kappa|\sigma|, \tag{4}$$

where $\kappa > 0$ is a constant.

According to Equation 4, the terminal sliding-mode (TSM) controller is designed as

$$u = \frac{1}{g(\xi, \ x)}\left[-f(\theta, \ x)-\beta\frac{q}{p}e_1{}^{\frac{q}{p}-1}e_2-(L_d + \eta)\,\mathrm{sgn}(\sigma) + y_d^{(2)}\right], \tag{5}$$

where $\eta > 0$ is a constant. Analyzing the TSMC surface function (3), we can obtain the system state errors e_1 and e_2 with controller u converging to zero in finite time.

Observing the TSM controller in Equation 5, the second term $\beta\frac{q}{p}e_1{}^{\frac{q}{p}-1}e_2$, when the sliding mode $\sigma=0$, ie, $e_2 = -\beta e_1^{\frac{q}{p}}$, substituting $e_2 = -\beta e_1^{\frac{q}{p}}$ into $e_1{}^{\frac{q}{p}-1}e_2$ then for the term of $-\beta e_1{}^{\frac{2q}{p}-1}$, if $q<p<2q$, $e_1{}^{\frac{q}{p}-1}e_2$ is nonsingular. When the system states reach the sliding-mode surfaces $\sigma = \dot{\sigma} = 0$, Equation 3 is described as follows:

$$\dot{e}_2 = -\beta e_1^{\frac{q}{p}}. \tag{6}$$

Suppose the arriving time is $t_s$from the initial state error $e_1(0)\neq0$ to $e_1(t_s)=0$. We have the integration of Equation 6 as

$$\int_{e_1(0)}^{e_1(t_s)} e_1{}^{-\frac{q}{p}}de_1 = \int_0^{t_s}-\beta dt. \tag{7}$$

Then

$$t_s = \frac{p}{\beta(p-q)}|e_1(0)|^{1-\frac{q}{p}}. \tag{8}$$

Remark 1. The convergence time will increase resulting from the nonlinear term $\beta e_1^{\frac{q}{p}}$, and the system states converge slowly in the regions approaching the equilibrium point, because the exponent of e_1 is less than 1 in Equation 3.

Remark 2. The switching gain η is generally chosen to be a larger value to achieve a faster convergence in TSM controller Equation 5, resulting in the chattering which affects the tracking precision and stability. It is also insufficient control for the systems with unknown system states and parameters in engineering applications.

Therefore, it is necessary to improve system convergence and eliminate system chattering based on the conventional TSM controller.

3 | FTSMC WITH DE USING ICD

Aim to solve the tracking control problems for the uncertain nonlinear system with unknown system states and unknown parameters and time-varying disturbances. A fast terminal sliding-mode finite-time tracking control scheme based on the differentiator evolution optimization algorithm using ICD is proposed to obtain faster convergence properties with high tracking precision.

To facilitate control system design, the following assumptions are presented in the subsequent developments.

Assumption 1. The desired trajectory $y_d(t)$ is differentiable with respect to time t and all of the higher-order derivatives are differentiable.

Assumption 2. Given the control input u is bounded, there exist constants l_g, $l_f \in R^+$ such that

$$\left|g(\hat{\xi},\hat{x})-g(\xi,x)\right| \le l_g\left\|\hat{\xi}-\xi\right\|\|\hat{x}-x\|. \tag{9}$$

Similarly,

$$\left|f(\hat{\theta},\hat{x})-f(\theta,x)\right| \le l_f\left\|\hat{\theta}-\theta\right\|\|\hat{x}-x\|. \tag{10}$$

Assumption 3. $\left|-f(\hat{\theta},\hat{x}) + {y_d}^{(2)} - \beta\frac{q}{p}\hat{e}_1{}^{\frac{q}{p}-1}\hat{e}_2 - \alpha\hat{e}_2\right| \le l_1$ is bounded[35] and $l_{\inf g} \le \left|g(\hat{\xi},\hat{x})\right| \le l_{\sup g}$.

3.1 | Integral chain differentiator

The FTSMC controller on the basis of a fast estimation scheme consists of an ICD and DE optimization. The ICD aims to estimate the unknown system states x_2 from the plant output $y = x_1$. For the proposed system, the estimation lemma is given as follows.

Lemma 1. (Liu and Wang[36]) *Consider nonlinear system (1) with the unknown states and unknown parameters, the ICD is designed by*

$$\begin{aligned}
\dot{\hat{x}}_1(t) &= \hat{x}_2(t),\\
\dot{\hat{x}}_2(t) &= \hat{x}_3(t),\\
\dot{\hat{x}}_3(t) &= -\frac{\gamma_1}{\omega^3}(\hat{x}_1(t)-x_1(t)) - \frac{\gamma_2}{\omega^2}\hat{x}_2(t) - \frac{\gamma_3}{\omega}\hat{x}_3(t),
\end{aligned} \tag{11}$$

where $\omega > 0$ is sufficiently small perturbation parameter. The differentiator is proposed to estimate $x_2(t)$ from the plant output $y = x_1(t)$. The speed parameters γ_1, γ_2, γ_3 are positive and chosen as the coefficients of Hurwitz polynomial such as $\sigma^3 + \gamma_3\sigma^2 + \gamma_2\sigma + \gamma_1 = 0$. Therefore, we have

$$\lim_{\omega\to 0}\hat{x}_i(t) = x_i(t),\ \ i = 1, 2. \tag{12}$$

and

$$\lim_{\omega\to 0}\hat{x}_3(t) = \lim_{\omega\to 0}\dot{\hat{x}}_2(t) = \dot{x}_2(t), \tag{13}$$

where $\hat{x}_i(t)\quad i = 1, 2, 3.$ are estimate system states.

The Laplace transformation of ICD is

$$\begin{aligned} &\hat{X}_{i-k}(s) = \frac{\hat{X}_i(s)}{s^k},\ \ k = 0,\ \ 1,\ \ 2;\ \ i = 1,\ \ 2,\ \ 3,\\ &s\hat{X}_3(s) + \frac{\gamma_3}{\omega}\hat{X}_3(s) + \frac{\gamma_2}{\omega^2}\hat{X}_2(s) + \frac{\gamma_1}{\omega^3}\hat{X}_1(s) = \frac{\gamma_1}{\omega^3}X_1(s), \end{aligned} \tag{14}$$

where $X_i(s)$ is the Laplace transformation of $\hat{x}_i(t),\ \ i = 1,\ \ 2,\ \ 3.$

Remark 3. From Equation 14, we have

$$\frac{\hat{X}_1(s)}{X_1(s)} = \frac{\frac{\gamma_1}{\omega^3}}{s^3 + \frac{\gamma_3}{\omega}s^2 + \frac{\gamma_2}{\omega^2}s^1 + \frac{\gamma_1}{\omega^3}} \tag{15}$$

It is noted that if the parameters $\gamma_1, \gamma_2, \gamma_3$ are chosen to be suitable, the filtering ability is able to be obtained.

3.2 | DE algorithm based on ICD

Differential evolution algorithms use a simple differential operator to create new candidate solutions and employ a one-to-one competition scheme to greedily select new candidates.[37] The DE using ICD realizes the parameters estimations with unknown system states. These unknown states in the systems are estimated by the differentiator using the only position signals of measurements. The key steps of DE algorithm are mutation, crossover, and selection. The initial individuals satisfying constraints are generated by adding uniformly distributed random deviations as Equation 16

$$x_{ij}(0) = rand_{ij}(0,\ \ 1)\left(x_{ij}{}^U - x_{ij}{}^L\right) + x_{ij}{}^L, \tag{16}$$

where $x_{ij}(t) i = 1, 2, 3,...,n, j = 1, 2, 3, \ldots, NP$, is each target vector, $x_{ij}{}^U$ and $x_{ij}{}^L$ are minimum and maximum values of the jth component respectively, $rand_{ij}(0,\ \ 1)$ is uniformly distributed random number in the range 0 to 1. Differential evolution algorithms generate a mutate vector by adding the weighted difference of 2 vectors to the third vector as Equation 17

$$h_{ij}(t+1) = x_{p_1 j}(t) + F\left(x_{p_2 j}(t) - x_{p_3 j}(t)\right). \tag{17}$$

The integer index randomly chooses as p_1, p_2, p_3 are mutually different and also chose to be different from the running index i referred to the ith candidate in the population consisting of n candidates and t is denoted the generation counter. The target vector in this case is a random individual $x_{p_1 j}(t)$, and $x_{p_2 j}(t)$ and $x_{p_3 j}(t)$ are 2 randomly selected individuals in the current population. The scale factor $F > 0$ controls the amplification level in the differential variation. The trial vector is defined component-wise as a binomial crossover operator as Equation 18

$$v_{ij}(t+1) = \begin{cases} h_{ij}(t+1), randl_{ij} \le CR \\ x_{ij}(t), \text{otherwise} \end{cases}, \tag{18}$$

where $randl_{ij}$ is a random number generated by using the uniform distribution in the range 0–1. The crossover constant $CR \in [0, 1]$ is to be determined by the user. If the trial vector is coming out to be better by the fitness function, the trial vector will replace the target vector, otherwise, $x_i(t)$ is selected to target vector which is defined as Equation 19.

$$x_i(t+1) = \begin{cases} v_i(t+1), f(v_i(t+1)) < f(x_i(t)) \\ x_i(t), \text{otherwise.} \end{cases} \tag{19}$$

Mutation, crossover, and selection will be operated repeatedly until the iteration reaches to the maximum iterations number G. The DE algorithm is depicted in Figure 1. To identify the unknown parameters, the system input signals will be rewritten as Equation 20

$$Y(t)\Theta(t) = \tau(t) \tag{20}$$

The identification criterion J is designed as Equation 21

$$J = \sum_{i=1}^{N} \frac{1}{2}(\tau_i - \hat{\tau}_i)^T(\tau_i - \hat{\tau}_i) \tag{21}$$

where N is the total number of data, optimization input test data denoted to τ_i, $i = 1, 2, \ldots, N$, and $\Theta(t) = \begin{bmatrix} \theta \\ \xi \end{bmatrix}$ is the identification parameter vector. When identification criterion J is sufficiently small, then we have $\lim_{J\to 0} \hat{\Theta}(t) = \Theta(t)$, ie, $\lim_{J\to 0} \hat{\theta} = \theta$, $\lim_{J\to 0} \hat{\xi} = \xi$..

3.3 | Fast terminal sliding-mode controller with DE using ICD and stability analysis

The FTSMC-DD objective is to track the desired trajectory of the uncertainty nonlinear system in high precision and steady by using differentiator based on DE algorithm. In this paper, the fast terminal sliding surface is defined as

$$\sigma(t) = e_2 + \alpha e_1 + \beta e_1^{\frac{q}{p}}. \tag{22}$$

Then, the estimate sliding surface is given by

$$\hat{\sigma}(t) = \hat{e}_2 + \alpha \hat{e}_1 + \beta \hat{e}_1^{\frac{q}{p}}, \tag{23}$$

where design parameters $\alpha > 0$, $\beta > 0$, $q < p < 2q, p, q$ are chosen to be odd integral $\bar{\beta} = \beta \frac{q}{p}$. The derivation with respect to time t on both sides of Equation 22 is obtained from

$$\dot{\sigma}(t) = \dot{e}_2 + \alpha \dot{e}_1 + \bar{\beta} e_1^{\frac{q}{p}-1} e_2. \tag{24}$$

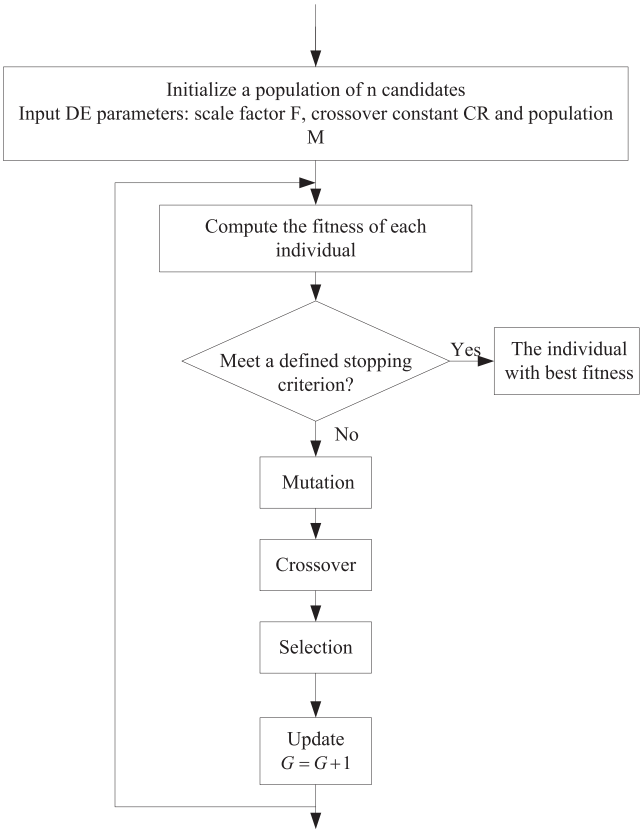

FIGURE 1 Differential evolution algorithm

Correspondingly,

$$\dot{\hat{\sigma}}(t) = \dot{\hat{e}}_2 + \alpha\dot{\hat{e}}_1 + \bar{\beta}\hat{e}_1^{\frac{q}{p}-1}\hat{e}_2. \tag{25}$$

To guarantee the tracking property, the fast terminal sliding tracking control system is given by the following theorem.

Theorem 1. *For system (1) with unknown system parameter vectors* θ, ξ *and unknown state* x_2 *and time-varying disturbances* $d(t)$*, the fast terminal sliding-mode tracking controller is designed as*

$$u(t) = \frac{1}{g(\hat{\xi},\hat{x})}\left(-f(\hat{\theta},\hat{x}) + y_d^{(2)}(t) - \bar{\beta}\hat{e}_1^{\frac{q}{p}-1}\hat{e}_2 - \alpha\hat{e}_2(t) - (L_d+\delta)\,\mathrm{sgn}(\hat{\sigma})\right). \tag{26}$$

Given to the high ICD using DE algorithm, the output signals will converge to the desired trajectory in finite time as follows

$$x_i(t) \to y_d^{(i-1)}(t), \quad i = 1, 2,$$

where the design parameter δ is chosen to be positive constant.

Proof. Consider a Lyapunov function candidate

$$V = \frac{1}{2}\sigma^2.$$

Its time derivative is

$$\dot{V} = \sigma\dot{\sigma}.$$

Furthermore, the derivation is

$$\begin{aligned}
\dot{V} &= \sigma\left(\dot{e}_2 + \alpha\dot{e}_1 + \bar{\beta}e_1^{\frac{q}{p}-1}e_2\right)\\
&= \sigma\left(\begin{array}{l} f(\theta,x) + d(t) + g(\xi,x)\dfrac{1}{g(\hat{\xi},\hat{x})}\left(\begin{array}{l} -f(\hat{\theta},\hat{x}) + y_d^{(2)}(t) - \bar{\beta}\hat{e}_1^{\frac{q}{p}-1}\hat{e}_2 \\ -\alpha\hat{e}_2(t) - (L_d+\delta)\,\mathrm{sgn}(\hat{\sigma}) \end{array}\right) \\ -y_d^{(2)}(t) + \alpha\dot{e}_1 + \bar{\beta}e_1^{\frac{q}{p}-1}e_2 \end{array}\right)\\
&= \sigma\left(\begin{array}{l} f(\theta,x) + d(t) + \dfrac{g(\hat{\xi},\hat{x}) + g(\xi,x) - g(\hat{\xi},\hat{x})}{g(\hat{\xi},\hat{x})}\left(\begin{array}{l} -f(\hat{\theta},\hat{x}) + y_d^{(2)}(t) - \bar{\beta}\hat{e}_1^{\frac{q}{p}-1}\hat{e}_2 \\ -\alpha\hat{e}_2(t) - (L_d+\delta)\,\mathrm{sgn}(\hat{\sigma}) \end{array}\right) \\ -y_d^{(2)}(t) + \alpha\dot{e}_1 + \bar{\beta}e_1^{\frac{q}{p}-1}e_2 \end{array}\right)\\
&= \sigma\left(\begin{array}{l} f(\theta,x) - f(\hat{\theta},\hat{x}) + d(t) - (L_d+\delta)\,\mathrm{sgn}(\hat{\sigma}) + \alpha(e_2-\hat{e}_2) + \bar{\beta}\left(e_1^{\frac{q}{p}-1}e_2 - \hat{e}_1^{\frac{q}{p}-1}\hat{e}_2\right) \\ +\dfrac{g(\xi,x) - g(\hat{\xi},\hat{x})}{g(\hat{\xi},\hat{x})}\left(\begin{array}{l} -f(\hat{\theta},\hat{x}) + y_d^{(2)}(t) - \bar{\beta}\hat{e}_1^{\frac{q}{p}-1}\hat{e}_2 \\ -\alpha\hat{e}_2(t) - (L_d+\delta)\,\mathrm{sgn}(\hat{\sigma}) \end{array}\right) \end{array}\right).
\end{aligned} \tag{27}$$

Next, Equation 28 is equivalent to the Equation 27 given by

$$\begin{aligned}
\dot{V} &= \sigma\left(f(\theta,x)-f\left(\hat{\theta},\hat{x}\right)\right)+\sigma(d(t)-(L_d+\delta)\,\mathrm{sgn}(\hat{\sigma}))+\sigma(\alpha(e_2-\hat{e}_2))\\
&+\sigma\left(\bar{\beta}\begin{pmatrix} e_1^{\frac{q}{p}-1} & e_2-\hat{e}_1^{\frac{q}{p}-1}\hat{e}_2\end{pmatrix}\right)+\sigma\frac{g(\xi,x)-g\left(\hat{\xi},\hat{x}\right)}{g\left(\hat{\xi},\hat{x}\right)}\begin{pmatrix} -f\left(\hat{\theta},\hat{x}\right)+y_d{}^{(2)}(t)-\bar{\beta}\hat{e}_1^{\frac{q}{p}-1}\hat{e}_2\\ -\alpha\hat{e}_2(t)-(L_d+\delta)\,\mathrm{sgn}(\hat{\sigma})\end{pmatrix}\\
&=\hat{\sigma}\left(f(\theta,x)-f\left(\hat{\theta},\hat{x}\right)\right)+(\sigma-\hat{\sigma})\left(f(\theta,x)-f\left(\hat{\theta},\hat{x}\right)\right)+\hat{\sigma}(\alpha(e_2-\hat{e}_2))\\
&+(\sigma-\hat{\sigma})(\alpha(e_2-\hat{e}_2))+\hat{\sigma}\left(\bar{\beta}\begin{pmatrix} e_1^{\frac{q}{p}-1} & e_2-\hat{e}_1^{\frac{q}{p}-1}\hat{e}_2\end{pmatrix}\right)+(\sigma-\hat{\sigma})\left(\bar{\beta}\begin{pmatrix} e_1^{\frac{q}{p}-1} & e_2-\hat{e}_1^{\frac{q}{p}-1}\hat{e}_2\end{pmatrix}\right)\\
&+\hat{\sigma}\frac{g(\xi,x)-g\left(\hat{\xi},\hat{x}\right)}{g\left(\hat{\xi},\hat{x}\right)}\begin{pmatrix} -f\left(\hat{\theta},\hat{x}\right)+y_d{}^{(2)}(t)-\bar{\beta}\hat{e}_1^{\frac{q}{p}-1}\hat{e}_2\\ -\alpha\hat{e}_2(t)-(L_d+\delta)\,\mathrm{sgn}(\hat{\sigma})\end{pmatrix}\\
&+(\sigma-\hat{\sigma})\frac{g(\xi,x)-g\left(\hat{\xi},\hat{x}\right)}{g\left(\hat{\xi},\hat{x}\right)}\begin{pmatrix} -f\left(\hat{\theta},\hat{x}\right)+y_d{}^{(2)}(t)-\bar{\beta}\hat{e}_1^{\frac{q}{p}-1}\hat{e}_2\\ -\alpha\hat{e}_2(t)-(L_d+\delta)\,\mathrm{sgn}(\hat{\sigma})\end{pmatrix}\\
&+\hat{\sigma}(d(t)-(L_d+\delta)\,\mathrm{sgn}(\hat{\sigma}))+(\sigma-\hat{\sigma})(d(t)-(L_d+\delta)\,\mathrm{sgn}(\hat{\sigma})).
\end{aligned}\tag{28}$$

Hence, Equation 29 is obtained.

$$\begin{aligned}
\dot{V}\leq\ & |\hat{\sigma}|\left|\left(f(\theta,x)-f\left(\hat{\theta},\hat{x}\right)\right)\right|+|(\sigma-\hat{\sigma})|\left|\left(f(\theta,x)-f\left(\hat{\theta},\hat{x}\right)\right)\right|+|\hat{\sigma}||\alpha||e_2-\hat{e}_2|\\
&+|\sigma-\hat{\sigma}||\alpha||e_2-\hat{e}_2|+|\hat{\sigma}||\bar{\beta}|\left|e_1^{\frac{q}{p}-1}\quad e_2-\hat{e}_1^{\frac{q}{p}-1}\hat{e}_2\right|+|\sigma-\hat{\sigma}||\bar{\beta}|\left|e_1^{\frac{q}{p}-1}\quad e_2-\hat{e}_1^{\frac{q}{p}-1}\hat{e}_2\right|\\
&+|\hat{\sigma}|\left|\frac{g(\xi,x)-g\left(\hat{\xi},\hat{x}\right)}{g\left(\hat{\xi},\hat{x}\right)}\right|\left|\begin{matrix} -f\left(\hat{\theta},\hat{x}\right)+y_d{}^{(2)}(t)-\bar{\beta}\hat{e}_1^{\frac{q}{p}-1}\hat{e}_2\\ -\alpha\hat{e}_2(t)-(L_d+\delta)\,\mathrm{sgn}(\hat{\sigma})\end{matrix}\right|\\
&+|(\sigma-\hat{\sigma})|\left|\frac{g(\xi,x)-g\left(\hat{\xi},\hat{x}\right)}{g\left(\hat{\xi},\hat{x}\right)}\right|\left|\begin{matrix} -f\left(\hat{\theta},\hat{x}\right)+y_d{}^{(2)}(t)-\bar{\beta}\hat{e}_1^{\frac{q}{p}-1}\hat{e}_2\\ -\alpha\hat{e}_2(t)-(L_d+\delta)\,\mathrm{sgn}(\hat{\sigma})\end{matrix}\right|\\
&+|d(t)||\sigma-\hat{\sigma}|+(L_d+\delta)|\sigma-\hat{\sigma}|-\delta|\hat{\sigma}|\\
\leq&|\hat{\sigma}|l_f\left\|\hat{\theta}-\theta\right\|\|\hat{x}(t)-x(t)\|+|\sigma-\hat{\sigma}|l_f\left\|\hat{\theta}-\theta\right\|\|\hat{x}(t)-x(t)\|+|\hat{\sigma}||\alpha||e_2-\hat{e}_2|\\
&+|\sigma-\hat{\sigma}||\alpha||e_2-\hat{e}_2|+|\hat{\sigma}||\bar{\beta}|\left|e_1^{\frac{q}{p}-1}\quad e_2-\hat{e}_1^{\frac{q}{p}-1}\hat{e}_2\right|+|(\sigma-\hat{\sigma})||\bar{\beta}|\left|e_1^{\frac{q}{p}-1}\quad e_2-\hat{e}_1^{\frac{q}{p}-1}\hat{e}_2\right|\\
&+|\hat{\sigma}|\frac{l_g\left\|\hat{\xi}-\xi\right\|\|\hat{x}(t)-x(t)\|}{l_{\inf g}}\left|\begin{matrix} -f\left(\hat{\theta},\hat{x}\right)+y_d{}^{(2)}(t)-\bar{\beta}\hat{e}_1^{\frac{q}{p}-1}\hat{e}_2\\ -\alpha\hat{e}_2(t)-(L_d+\delta)\,\mathrm{sgn}(\hat{\sigma})\end{matrix}\right|\\
&+|\sigma-\hat{\sigma}|\frac{l_g\left\|\hat{\xi}-\xi\right\|\|\hat{x}(t)-x(t)\|}{l_{\inf g}}\left|\begin{matrix} -f\left(\hat{\theta},\hat{x}\right)+y_d{}^{(2)}(t)-\bar{\beta}\hat{e}_1^{\frac{q}{p}-1}\hat{e}_2\\ -\alpha\hat{e}_2(t)-(L_d+\delta)\,\mathrm{sgn}(\hat{\sigma})\end{matrix}\right|\\
&+|d(t)||\sigma-\hat{\sigma}|+(L_d+\delta)|\sigma-\hat{\sigma}|-\delta|\hat{\sigma}|
\end{aligned}\tag{29}$$

Using the Equation 21, we have $\hat{\tau}\to\tau$, when J is sufficiently small.

According to the Equation 20, the result is obtained as

$$\lim_{J\to 0}\hat{\Theta}(t)=\Theta(t),$$

where $\Theta(t)=\begin{bmatrix}\theta\\ \xi\end{bmatrix}$ is unknown parameters vectors.

Equivalently,

$$\lim_{J\to 0}\hat{\theta}=\theta,\quad \lim_{J\to 0}\hat{\xi}=\xi$$

and

$$\lim_{J\to 0}\left\|\hat{\theta}-\theta\right\|=0,\qquad \lim_{J\to 0}\left\|\hat{\xi}-\xi\right\|=0,$$

when perturbation parameter ω is sufficiently small and according to the result in *Lemma* 1, we have

$$\lim_{\omega\to 0}|\hat{x}_i-x_i|=0\qquad i=1,2.$$

According to Equation 12, we have

$$\lim_{\omega\to 0}\hat{e}_1=\lim_{\omega\to 0}(\hat{x}_1-y_d)=e_1,\ \lim_{\omega\to 0}\hat{e}_2=\lim_{\omega\to 0}(\hat{x}_2-\dot{y}_d)=e_2.$$

Using Equations 22 and 23, we have

$$\lim_{\omega\to 0}|\sigma-\hat{\sigma}|=0.$$

Consequently, $\dot{V}\leq-\delta|\hat{\sigma}|\leq 0$ ie, $\dot{V}=\sigma\dot{\sigma}\leq 0$ and $x_i(t)\to {y_d}^{(i-1)}(t)$, $i=1,2$, which proves the results. The tracking systems are stable with tracking errors converging to the origin.

When the exponent of position tracking errors e_1 is less than 1, ${e_1}^{\frac{q}{p}-1}$ will converge in nonlinearity. Apparently, the convergence speed in the nonlinear form of ${e_1}^{\frac{q}{p}-1}$ is slower than that in the linear form of e_1. Although the system is disturbed by time-varying signals$d(t)$, which exaggerates the tracking errors, the estimate signal $\hat{e}_2$ is filtered by the differentiator, which is robust to the disturbances. It is feasible that the speed tracking errors $\hat{e}_2$ without the noise disturbances will be estimated accurately faster by adjusting the speeding parameters and perturbation parameters.

The following analysis is provided to demonstrate the finite-time attainability of sliding-mode surface. When the system states reach the sliding-mode surface $\hat{\sigma}=\dot{\hat{\sigma}}=0$, Equation 23 is described as follows:

$$\hat{e}_2=-\alpha\hat{e}_1-\beta{\hat{e}_1}^{\frac{q}{p}}. \tag{30}$$

Suppose the arriving time is t_s from the initial state error $\hat{e}_1(0)\neq 0$ to $\hat{e}_1(t_s)=0$. We have the integration of Equation 30 as

$$\int_{\hat{e}_1(0)}^{\hat{e}_1(t_s)}\frac{1}{-\alpha\hat{e}_1-\beta{\hat{e}_1}^{\frac{q}{p}}}d\hat{e}_1=\int_0^{t_s}dt. \tag{31}$$

Then

$$t_s=\frac{p}{\alpha(p-q)}\ln\frac{\alpha\hat{e}_1(0)^{1-\frac{q}{p}}+\beta}{\beta}. \tag{32}$$

It can be concluded that the system tracking errors arrive at the sliding-mode surface in finite time from Equation 32.

4 | SIMULATION

The uncertain nonlinear systems with time-varying disturbances are presented to illustrate the validity of the proposed approach. The uncertain systems are required to reach and maintain the desired trajectory in finite time. Consider the following inverted pendulum systems as

$$\begin{cases} \dot{x}_1 = x_2 \\ \dot{x}_2 = \dfrac{g\sin x_1 - mlx_2^2\cos x_1\sin x_1/(m_c+m)}{l(4/3 - m\cos^2 x_1/(m_c+m))} + \dfrac{\cos x_1/(m_c+m)}{l(4/3 - m\cos^2 x_1/(m_c+m))}u + d(t) \end{cases}.$$

The unknown parameters m_c, m, l are identified through FTSMC using DE algorithm based on ICD. Optimization processing of the identification criterion J is presented in Figure 2. In this case, the ICD parameters are selected to be $\omega = 0.01$, $\gamma_1 = 10, \gamma_2 = \gamma_3 = 15$. The scale factor of DE identification is $F = 0.6$. The crossover probability is chosen to be CR = 0.5 and the size of the population is 90. The maximum number of iteration is 200 and the true value of identification parameters are$m_c = 1.5$, $m = 0.4$, $l = 0.6$. For parameters identification simplicity, we transform the parameters in the form as $\Theta_1 = (m_c + m)\frac{4}{3}l$, $\Theta_2 = (m_c + m)g$, $\Theta_3 = ml$.

The identification results are $\Theta_1 = 1.5191$, $\Theta_2 = 18.6116$, $\Theta_3 = 0.2414$. Its corresponding system parameters are $\hat{m}_c = 1.4968$, $\hat{m} = 0.4024$, $\hat{l} = 0.5999$ identification criterion$Best\,J = 1.34 \times 10^{-2}$.

$$u(t) = \frac{1}{g(\hat{\xi}, \hat{x})}\left(-f(\hat{\theta}, \hat{x}) + y_d^{(2)}(t) - \beta\frac{q}{p}\hat{e}_1(t)^{\frac{q}{p}-1}\hat{e}_2(t) - \alpha\hat{e}_2(t) - (L_d + \delta)\,\mathrm{sgn}(\hat{\sigma})\right)$$

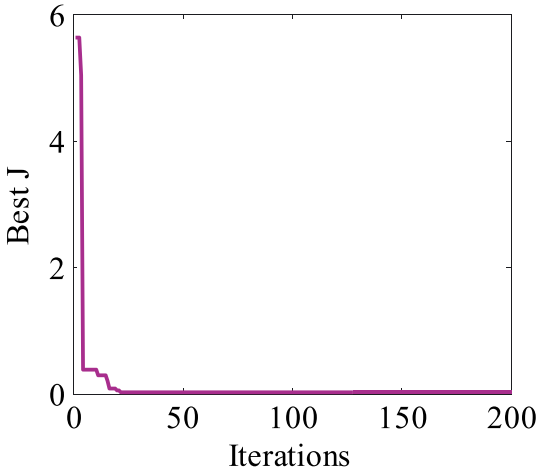

FIGURE 2 Optimization of the identification criterion J in inverted pendulum system [Colour figure can be viewed at wileyonlinelibrary.com]

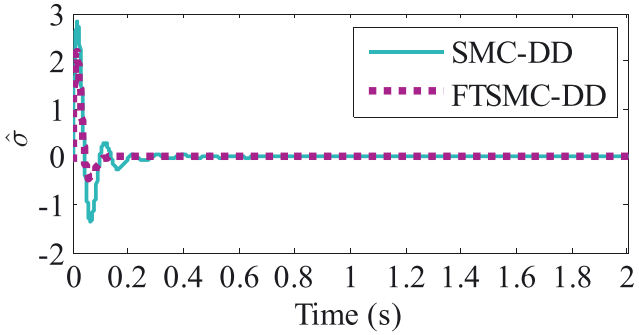

FIGURE 3 Fast terminal sliding-mode control–based differential evolution optimization algorithm using integral chain differentiator sliding-mode variable [Colour figure can be viewed at wileyonlinelibrary.com]

The simulation is implemented with the desired trajectory $y_d = 0.1 \sin t, g = 9.8$, time-varying disturbances $d(t) = 0.3 \sin t$ and parameters as $p = 9$, $q = 7$, $\alpha = 0.5$, $\beta = 2$, $L_d = 0.3$, $\delta = 3$.

The sliding-mode variable of proposed FTSM control based on the exponent reaching la method compared with the SMC manifold variable is shown in Figure 3. It is clear to see FTSMC-DD has a faster convergence with light fluctuations compared with the SMC-DD in sliding-mode manifold with intense oscillation. Figures 4 and 5 shows the inverted pendulum system control input signals using SMC-DD and FTSMC-DD respectively. The FTSMC-DD input signal obtains an effect control without chattering by the fast finite-time control. Although the differentiator has the filter function, SMC-DD has an impact on control signals with constant chattering because of the time-varying disturbances.

Figure 6 shows the position tracking versus time, which can be seen from that, the position output signals tracks the desired trajectory in high precision. The speed estimation results are shown in Figure 7, which demonstrates the accuracy of tracking trajectory to the reference signals.

The estimated state $\hat{x}_2$ is displayed in Figure 8. Although system states are disturbed by the time-varying noises signals and system parameters are unknown, the system state x_2 is estimated accurately using the ICD based on the DE algorithm. It verifies the ICD robustness and strong filter function. It is noted that fast terminal sliding mode control with the integral chain differentiator using DE algorithm not only could estimate the unknown parameters and states, but also extra and additionally could provide an accurate approximate for $f(\hat{\theta}, \hat{x})$ clearly shown as in Figure 9.

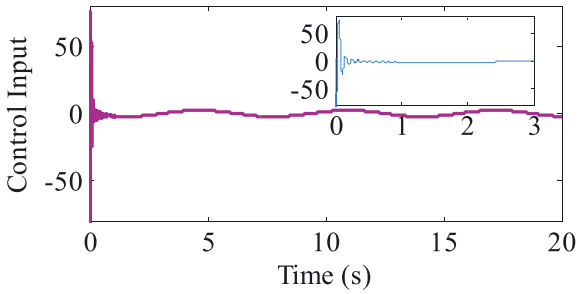

FIGURE 4 Control input signals using sliding-mode control–based differential evolution optimization algorithm using integral chain differentiator [Colour figure can be viewed at wileyonlinelibrary.com]

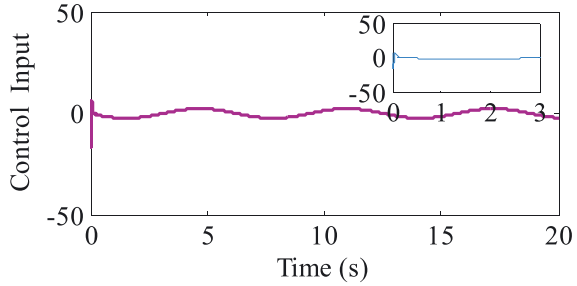

FIGURE 5 Fast terminal sliding-mode control–based differential evolution optimization algorithm using integral chain differentiator control input [Colour figure can be viewed at wileyonlinelibrary.com]

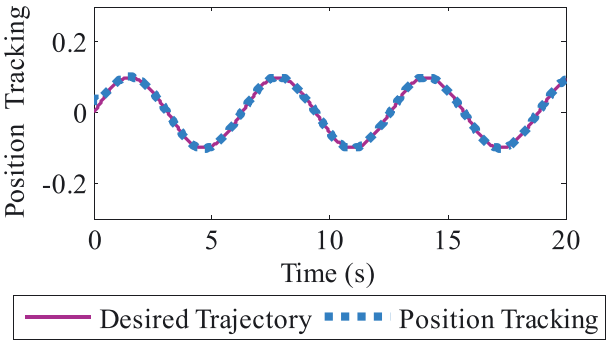

FIGURE 6 Position tracking [Colour figure can be viewed at wileyonlinelibrary.com]

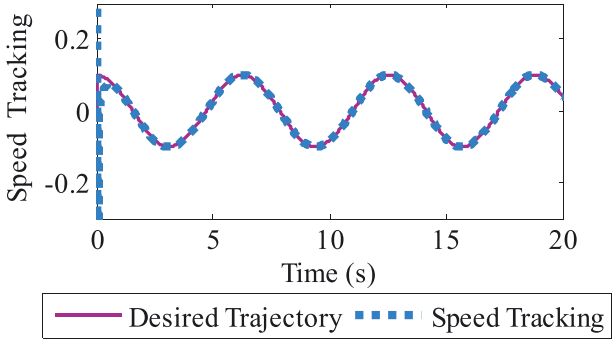

FIGURE 7 Speed tracking [Colour figure can be viewed at wileyonlinelibrary.com]

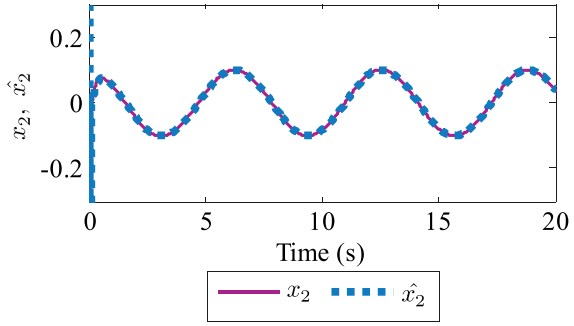

FIGURE 8 State x_2 and estimated value [Colour figure can be viewed at wileyonlinelibrary.com]

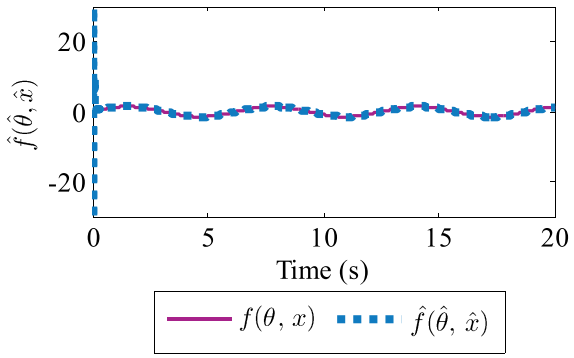

FIGURE 9 Estimated $f(\theta, x)$ [Colour figure can be viewed at wileyonlinelibrary.com]

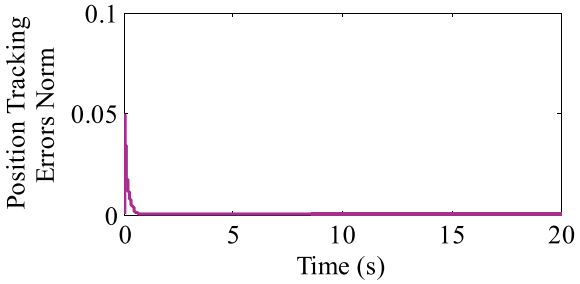

FIGURE 10 Fast terminal sliding-mode control–based differential evolution optimization algorithm using integral chain differentiator estimated position tracking error norm [Colour figure can be viewed at wileyonlinelibrary.com]

Figure 10 demonstrates that estimated position tracking errors converge to zero rapidly in a short tracking period. The converge results can be seen in Figure 11, which shows that the estimated speed tracking error norm more rapidly converges to the origin as compared with estimated position tracking error convergence, which verifies the precision tracking performance by the FTSMC-DD approach.

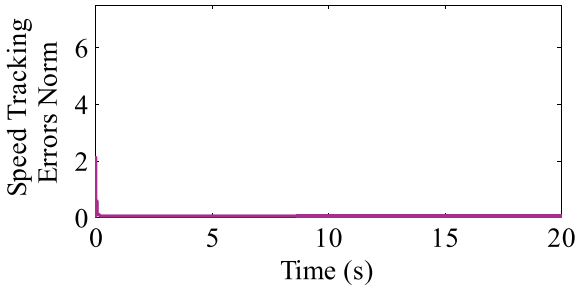

FIGURE 11 Fast terminal sliding-mode control–based differential evolution optimization algorithm using integral chain differentiator estimated speed tracking error norm [Colour figure can be viewed at wileyonlinelibrary.com]

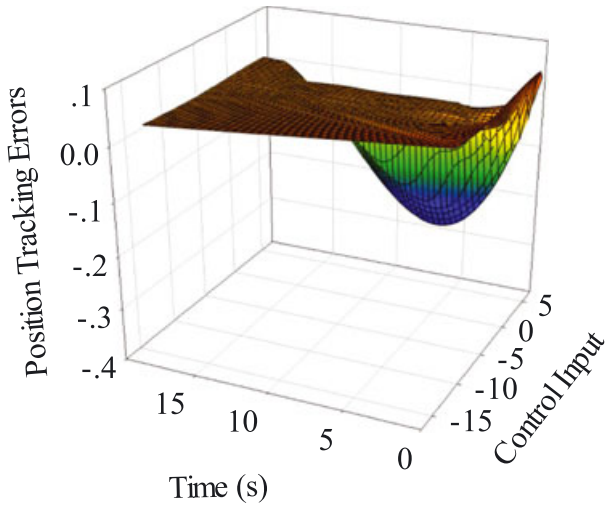

FIGURE 12 Fast terminal sliding-mode control–based differential evolution optimization algorithm using integral chain differentiator position tracking errors and control input [Colour figure can be viewed at wileyonlinelibrary.com]

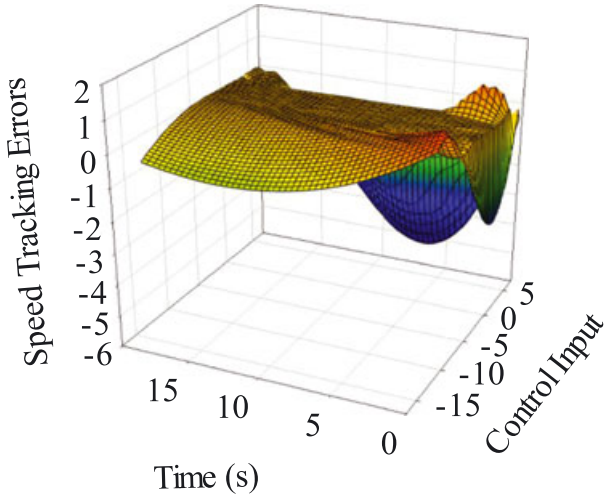

FIGURE 13 Fast terminal sliding-mode control–based differential evolution optimization algorithm using integral chain differentiator speed tracking errors and control input [Colour figure can be viewed at wileyonlinelibrary.com]

To illustrate the high-precision tracking performances of position and speed trajectory tracking without a chattering effect, the dynamic of control input signals with position and speed tracking errors within the tracking period is shown in Figures 12 and 13, respectively. It is clear that the position tracking errors and speed tracking errors converge to the central areas and the surface is smooth without steep oscillations. It is verified that the position and speed signals track the desired trajectory steadily.

5 | CONCLUSION

In this paper, an FTSMC combined with a DE algorithm and an ICD is proposed to solve tracking problems for a class of uncertain nonlinear systems with unknown parameters, unknown system states, and time-varying disturbances. The integration of the DE algorithm using ICD to the design of the sliding-mode controller estimates the unknown parameters, avoiding the unknown state limitation. The unknown system states of the uncertain nonlinear system are estimated by the design of the ICD added into the feedback in the tracking system. The technique of combing a DE algorithm and ICD into FTSMC is provided to realize track trajectory with unknown parameters and states with time-varying disturbances. Although the interference from time-varying disturbances exaggerates the tracking errors and chattering phenomenon, the differentiator filter function eliminates the disturbance effect and reduces the chattering in large scale. Compared with the conventional SMC, the algorithm proposed completes a fast global tracking error convergence without chattering, which obtains more rapidly and steadily precision tracking. The stability of the closed-loop system is proven based on the Lyapunov approach. Tracking errors are driven to the sliding-mode surface to converge to the origin in a finite time. The simulation results exhibit high-precision output tracking performance.

ACKNOWLEDGEMENT

This work was supported by the National Natural Science Foundation of China, under grant 61473202.

REFERENCES

1. Utkin VI. *Sliding Modes in Control and Optimization*. Berlin: Springer-Verlag; 2008.
2. Edwards C, Spurgeon S. *Sliding Mode Control: Theory and Applications*. London, UK: Taylor and Francis; 1998.
3. Zhao DY, Zhu QM. Position synchronized control of multiple robotic manipulators based on integral sliding mode. *Int J Syst Sci*. 2014;45(3):556-570.
4. Li H, Yu J, Hilton C, Liu H. Adaptive sliding-mode control for nonlinear active suspension vehicle systems using T–S fuzzy approach. *IEEE Trans Ind Electron*. 2013;60(8):3328-3338.
5. Orlowska-Kowalska T, Dybkowski M, Szabat K. Adaptive sliding-mode neuro-fuzzy control of the two-mass induction motor drive without mechanical sensors. *IEEE Trans Ind Electron*. 2010;57(2):553-564.
6. Dybkowski M, Orlowska-Kowalska T, Tarchala G. Sensorless traction drive system with sliding mode and MRAS(CC) estimators using direct torque control. *Automatika*. 2013;54(3):329-336.
7. Vrdoljak K, Peric N, Petrovic I. Applying optimal sliding mode based load-frequency control in power systems with controllable hydropower plants. *Automatika*. 2010;51(1):3-18.
8. Pukdeboon C. Inverse optimal sliding mode control of spacecraft with coupled translation and attitude dynamics. *Int J Syst Sci*. 2015;46(13):2421-2438.
9. Padhye N, Bhardawaj P, Deb K. Improving differential evolution through a unified approach. *J Glob Optim*. 2013;55(4):771-799.
10. Chen PC, Chen CW, Chiang WL. Linear matrix inequality conditions of nonlinear systems by genetic algorithm-based H-infinity adaptive fuzzy sliding mode controller. *J Vib Control*. 2011;17(2):163-173.
11. Saoudi K, Harmas MN, Bouchama Z. Design of a robust and indirect adaptive fuzzy sliding mode power system stabilizer using particle swarm optimization. *Energy Sources Part A—Recovery Utilization and Environmental Effects*. 2014;36(15):1670-1680.
12. Djari A, Bouden T, Boulkroune A. Design of fractional-order sliding mode controller (FSMC) for a class of fractional-order nonlinear commensurate systems using a particle swarm optimization (PSO) algorithm. *Control Eng Appl Inf*. 2014;16(3):46-55.
13. Banerjee A, Abu-Mahfouz I. A comparative analysis of particle swarm optimization and differential evolution algorithms for parameter estimation in nonlinear dynamic systems. *Chaos Solitons Fractals*. 2014;58:65-83.
14. Civicioglu P, Besdok E. A conceptual comparison of the cuckoo-search, particle swarm optimization, differential evolution, and artificial bee colony algorithms. *Artif Intell Rev*. 2013;39(4):315-346.

15. Ghosh S, Das S, Vasilakos AV, Suresh K. On convergence of differential evolution over a class of continuous functions with unique global optimum. *IEEE Trans Syst Man Cybern Part B—Cybernetics*. 2012;42(1):107-124.
16. Vardakos S, Gutierrez M, Xia C. Parameter identification in numerical modeling of tunneling using the differential evolution genetic algorithm (DEGA). *Tunn Undergr Space Technol*. 2012;28:109-123.
17. Chakraborty J, Konar A, Jain LC, Chakraborty UK. Cooperative multi-robot path planning using differential evolution. *J Intell Fuzzy Syst*. 2009;20(1–2):13-27.
18. Marcic T, Stumberger B, Stumberger G. Differential-evolution-based parameter identification of a line-start IPM synchronous motor. *IEEE Trans Ind Electron*. 2014;61(11):5921-5929.
19. Tang YG, Zhang XY, Hua CC, Li LX, Yang YX. Parameter identification of commensurate fractional-order chaotic system via differential evolution. *Phys Lett A*. 2012;376(4):457-464.
20. Li SH, Ding SH, Li Q. Global set stabilization of the spacecraft attitude control problem based on quaternion. *Int J Robust Nonlinear Control*. 2010;20:84-105.
21. Wu YQ, Yu XH, Man ZH. Terminal sliding mode control design for uncertain dynamic systems. *Syst Control Letters*. 1998;34:281-287.
22. Feng Y, Han F, Yu X, Stonier D, Man Z. 'Finite time stability of homogeneous systems,' The 6th IEEE International Workshop on Variable Structure Systems, Singapore, 2000; 325–334.
23. Hong YG, Jiang ZP. Finite-time stabilization of nonlinear systems with parametric and dynamic uncertainties. *IEEE Trans Autom Control*. 2006;51:1950-1956.
24. Rahmani M, Ghanbari A, Ettefagh MM. Hybrid neural network fraction integral terminal sliding mode control of an inchworm robot manipulator. *Mech Syst Sig Process*. 2016;80:117-136.
25. Gudey SK, Gupta R. Recursive fast terminal sliding mode control in voltage source inverter for a low-voltage microgrid system. *IET Gener Transm Distrib*. 2016;10:1536-1543.
26. Patnaik RK, Dash PK. Fast adaptive back-stepping terminal sliding mode power control for both the rotor-side as well as grid-side converter of the doubly fed induction generator-based wind farms. *IET Renew Power Gener*. 2016;10:598-610.
27. Efimov DV, Fridman L. A hybrid robust non-homogeneous finite-time differentiator. *IEEE Trans Autom Control*. 2011;56(5):1213-1219.
28. Wang XH, Chen ZQ, Yang G. Finite-time-convergent differentiator based on singular perturbation technique. *IEEE Trans Autom Control*. 2007;52(9):1731-1737.
29. Shao XL, Wang HL. Back-stepping robust trajectory linearization control for hypersonic reentry vehicle via novel tracking differentiator. *J Franklin Inst—Eng Appl Math*. 2016;353(9):1957-1984.
30. Xiong JJ, Zhang GB. Global fast dynamic terminal sliding mode control for a quadrotor UAV. *ISA Trans*. 2017;66:233-240.
31. Qiu ZC, Zhang SM. Fuzzy fast terminal sliding mode vibration control of a two-connected flexible plate using laser sensors. *J Sound Vib*. 2016;380:51-77.
32. Yazici I, Yaylaci EK. Fast and robust voltage control of DC–DC boost converter by using fast terminal sliding mode controller. *IET Power Electron*. 2016;9(1):120-125.
33. Hong MZ, Paplinski AP, Wu HR. A robust MIMO terminal sliding mode control scheme for rigid robotic manipulators. *IEEE Trans Autom Control*. 1994;39(12):2464-2469.
34. Utkin VI. *Sliding Modes in Control Optimization*. Berlin, Heidelberg: Springer; 1992.
35. Slotine JJE, Li WP. *Applied Nonlinear Control*. Prentice-Hall; 1991.
36. Liu JK, Wang XH. *Advanced Sliding Mode Control for Mechanical Systems: Design, Analysis and MATLAB Simulation*. Springer and Tsinghua University Press; 2011.
37. Rainer S, Kenneth P. Differential evolution - A simple and efficient heuristic for global optimization over continuous spaces. *Journal of Global Optimization*. 1997;11:341-359.

How to cite this article: Ma R, Zhang G, Krause O. Fast terminal sliding-mode finite-time tracking control with differential evolution optimization algorithm using integral chain differentiator in uncertain nonlinear systems. *Int J Robust Nonlinear Control*. 2017;1–15. https://doi.org/10.1002/rnc.3890